Available online at www.sciencedirect.com
ScienceDirect
Journal of Solid State Chemistry 181 (2008) 593–602
JOURNAL OF SOLID STATE CHEMISTRY
www.elsevier.com/locate/jssc

Visible-light responsive dye-modified TiO_2 photocatalyst

Dong Jiang[a,b], Yao Xu[a,*], Dong Wu[a], Yuhan Sun[a,**]

[a]State Key Laboratory of Coal Conversion, Institute of Coal Chemistry, Chinese Academy of Sciences, Taiyuan 030001, PR China
[b]Graduate University of the Chinese Academy of Sciences, Beijing 100049, PR China

Received 1 November 2007; received in revised form 29 December 2007; accepted 6 January 2008
Available online 10 January 2008

Abstract

A series of dye-modified TiO_2 photocatalysts were synthesized using dye Chrysoidine G (CG), tolylene-2,4-diisocyanate (TDI), and commercial TiO_2 (Degussa P25) as starting materials. TDI was used as a bridging molecule whose two –NCO groups reacted with Ti–OH of TiO_2 and $–NH_2$ groups of CG, respectively. As a result, special organic complexes were formed on the TiO_2 surface via stable π-conjugated chemical bonds between TiO_2 and dye molecules, confirmed by FT-IR, XPS, and UV–vis spectra. Due to the existence of π-conjugated surface organic complexes, the as-synthesized photocatalysts showed a great improvement in visible absorption (400–550 nm). Methylene blue, as a photodegradation target, was used to evaluate the photocatalytic performance, and the dye-modified TiO_2 exhibited much better activity under the visible light irradiation than bare TiO_2.

Keywords: TiO_2; Dye-modified; Photocatalytic activity

1. Introduction

Titanium dioxide (TiO_2) as a photocatalyst for degrading organic pollutions has attracted much attention because of its various advantages [1]. Unfortunately, the technological use of TiO_2 is limited by its wide band gap (3.2 eV for anatase), which requires UV light irradiation to obtain its photocatalytic activity. Because UV light only accounts for a small fraction (5%) of the sun's energy compared to visible light (45%) [2], any attempt making TiO_2 absorb visible light will have a profound positive effect on its visible photocatalytic performance. For this purpose, various efforts have been directed toward the development of visible-light responsive TiO_2 materials.

One of the initial approaches to shift the optical response of TiO_2 from the UV to the visible region was the doping of TiO_2 with transition-metal ions [3–10]. However, the photocatalytic activity of metal doping was impaired by bad thermal stability [11] and increased carrier-recombination possibility [12]. Another approach, from which TiO_2 obtained the desired narrow band gap, was the doping of TiO_2 with non-metal elements including C, N, S, F, B, and I [13–28] or codoping with N and F [29,30]. By these above methods, the absorption edge of TiO_2 could shift to the visible region and the doped TiO_2 showed photocatalytic activities under visible light irradiation. But, the inorganic-modified TiO_2 could not adequately utilize visible light due to their poor visible absorption. Recently, more and more attention has been paid to organic modification on TiO_2 surface to prepare visible-light responsive TiO_2 photocatalysts. Generally, there were two types of organic modification methods. One was based on the chemical/physical adsorption of dye molecules on TiO_2 surface for construction of dye-sensitized photocatalysts that could work under visible light irradiation [31–33]. Another approach utilized the chemical reaction betweean Ti–OH and phenolic hydroxyl of organic compounds (not dye), such as catechol [34,35], salicylic [36], and binaphthol [37], to form surface complexes on TiO_2 surface and to realize visible light absorption. So-produced organic-modified TiO_2 was also a visible light activated photocatalyst [37]. However, there were some disadvantages in above-mentioned organic-modified methods. As to the dye-sensitized TiO_2

*Corresponding author. Fax: +86 351 4041153.
**Also to be corresponded.
E-mail addresses: xuyao@sxicc.ac.cn (Y. Xu), yhsun@sxicc.ac.cn (Y. Sun).

0022-4596/$ - see front matter © 2008 Elsevier Inc. All rights reserved.
doi:10.1016/j.jssc.2008.01.004

photocatalysts, the dye molecules were only adsorbed on TiO_2 surface and no stable chemical bonds were formed between them. As a result, the dye molecules were easy to desorb from TiO_2 surface during photocatalytic process, which could decrease its photocatalytic activity. For the later method, although organic molecules were grafted on TiO_2 surface via firm covalent bonds, the obtained organic-modified TiO_2 showed very weak absorption in visible region. Thus, if a synthetic strategy could inherit all the advantages of above two methods, it could be very desirable to enhance the visible photocatalytic performance of TiO_2.

Here, a simple organic reaction was utilized to synthesize a visible-light responsive TiO_2 photocatalyst. It was well known that the Ti–OH on TiO_2 surface could react with isocyanate (–NCO). In our previous work, tolylene-2,4-diisocyanate (TDI) was used to modified TiO_2 to synthesize TDI-modified TiO_2 photocatalysts. Interestingly, the obtained photocatalysts showed good visible photocatalytic activity [38]. In the present work, a dye-modified TiO_2 photocatalyst was synthesized using dye Chrysoidine G, TDI, and Degussa P25 as raw materials. The photocatalytic activity of dye-modified TiO_2 photocatalyst was evaluated by degrading methylene blue (MB) under visible irradiation. The visible photocatalytic activity was correlated with the surface organic complex formation that was supported by the UV–vis diffuse reflectance spectra (DRS). The influencing factors of visible photocatalytic performance were also discussed.

2. Experimental section

2.1. Materials and regents

Dichloromethane (CH_2Cl_2, analytical reagent grade, Beijing Reagent Co.), triethylamine (Et_3N; analytical reagent grade, Beijing Reagent Co.) and tolylene-2,4-diisocyanate (TDI; +99.5%, Aldrich) were used without further purification. Original material TiO_2 was commercial Degussa P25 (75% anatase, 25% rutile, BET surface area: $\sim 50\,m^2\,g^{-1}$, size: ~ 30 nm). Dye Chrysoidine G ($CG \cdot HCl$, for microscopy, Fluka) was pretreated to obtained molecular CG before use as follows: (1) some amount of $CG \cdot HCl$ was dispersed in CH_2Cl_2 to form a suspension because $CG \cdot HCl$ could not dissolve in CH_2Cl_2, and then Et_3N was added into the suspension. The added Et_3N reacted with $CG \cdot HCl$ to produce $Et_3N \cdot HCl$ and CG. After stirred for 1 h, resultant CG gradually dissolved well into CH_2Cl_2 phase. The original $CG \cdot HCl/CH_2Cl_2$ suspension became a yellow-brown CG/CH_2Cl_2 solution with some $Et_3N \cdot HCl$ precipitation. (2) Some amount of water was added into above solution and then the solution was divided into two layers. The upper layer was aqueous solution of $Et_3N \cdot HCl$ and the lower layer was CH_2Cl_2 solution of CG. The organic layer was separated and collected. (3) The obtained CG/CH_2Cl_2 solution was dehydrated with anhydrous $MgSO_4$ powder. Thus, in this solution, dye CG existed as charge-neutral molecule not a hydrochloride. After filtered, the prepared CG/CH_2Cl_2 solution was directly used in next synthesis.

2.2. Preparation of dye-modified TiO_2

The whole preparation process of dye-modified TiO_2 might be preceded as shown in Scheme 1. In a typical synthetic procedure, 1.6 g (0.02 mol) of TiO_2 was dispersed into CH_2Cl_2 under magnetic stirring and formed a white suspension. After TDI was added dropwise into TiO_2/CH_2Cl_2 suspension under nitrogen, the suspension gradually turned to yellow, suggesting some chemical reaction had occurred between the TDI molecules and TiO_2 particles. The intermediate produced in this stage was designated as TP*X*, where *X* was the molar ratio of TDI/TiO_2. The formed TP*X* suspension in CH_2Cl_2 was stirred at room temperature for 2 h and subsequently filtered to obtain yellow TP*X* solid sample. To remove the adsorbed or unreacted TDI, the TP*X* solid sample was washed three

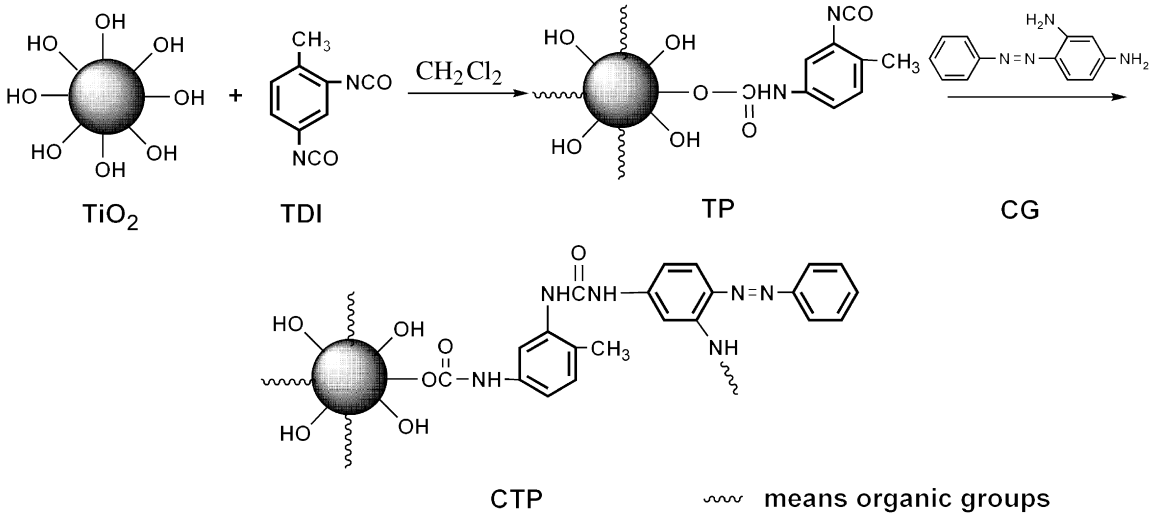

Scheme 1. Schematic illustration of the formation process of CTP.

times with CH_2Cl_2. Finally, the intermediate TP*X* was dried in a vacuum oven at 60 °C and then redispersed into CH_2Cl_2. The newly obtained TP*X* suspension was added into the pretreated CG/CH_2Cl_2 solution obtained in 2.1 with magnetic stirring under nitrogen. After 4-h reaction, the resulted product was filtrated and extracted for 48 h with CH_2Cl_2 to completely remove unreacted CG on TP*X* surface. Finally, the products were dried at 60 °C and denoted as CTP*X*, where *X* had the same meaning as that of TP*X*. During the whole preparation of catalysts, the molar ratio of CG/TDI were remained 0.5 and the content of TiO_2 was fixed at 1.6 g.

2.3. Characterization of samples

The crystalline phase of samples was determined by X-ray diffraction (XRD; Cu*K*α, 40 kV, 100 mA, D/max2500 Rigaku). The morphologies of samples were observed with transmission electron microscope (TEM; Hitachi-600-2). The BET surface area was measured by nitrogen adsorption at 77 K (Tristar3000, Micromeritics). The chemical structure information of samples was collected by FT-IR spectra (Nicolet 470 Spectrometer). The surface element composition and surface chemical state of samples were determined by X-ray photoelectron spectroscopy (XPS; Mg*K*α as radiation source, PHI-5300X, Perkin-Elmer Physics Electronics). UV–vis DRS and UV–vis absorption spectra were recorded on a Shimadzu UV-3150 apparatus. DRS was measured equipped with an integrating sphere, using $BaSO_4$ as reference.

2.4. Photodegradation of methylene blue (MB)

Photodegradation of MB was chosen to evaluate the photocatalytic performance of as-synthesized catalysts. The photocatalytic activities of dye-modified samples (CTP) and TiO_2 were studied by measuring the degradation of MB in aqueous–ethanol ($V_{water}/V_{ethanol} = 9$) mixture under the visible irradiation. The addition of ethanol was to improve the dispersibility of CTP samples. A 250-W metal halide lamp (Philips) was used as the light source and positioned inside a cylindrical Pyrex vessel surrounded by a circulating water jacket to cool the lamp. A UV-cutoff filter was placed between the Pyrex jacket and MB solution to remove UV radiation below 420 nm, ensuring that the photodegradation substrate was radiated only by visible light. The reaction system was composed of 250 mg of catalysts (TiO_2 or CTP) and 250 mL water–ethanol mixture containing MB with concentrations at 50 ppm (C_0). In all experiments, prior to irradiation, the catalyst suspension in MB solution was stirred in the dark for 30 min to achieve an MB adsorption/desorption equilibrium. The concentration of MB at this point was considered as the absorption equilibrium concentration C_e. The adsorption capacity of catalysts to MB was defined by the adsorption amount of MB on photocatalyst, which was equal to ($C_0 - C_e$). After 12-h visible light irradiation, the dispersion was sampled (4 mL), centrifuged, and filtered through a Millipore filter (pore size, 0.22 μm) to separate the catalysts particles. The filtrates were analyzed by UV–vis absorption spectra to determine the concentration of MB (*C*) after specialized 12-h reaction time. The degradation percentage of MB after 12-h irradiation was calculated by the formula: degradation percentage = $(1 - C/C_0) \times 100\%$. The stability of CTP catalysts were investigated by the circular photodegradation experiments that were carried out under the same reaction condition as mentioned above. Every time recycle finished, the used catalyst was centrifuged, washed with ethanol and dried before reuse. The recycled period was set to 12 h.

3. Results and discussion

3.1. Formation of dye-modified TiO_2

From Scheme 1, the synthetic process of CTP could be divided into two steps. In the first step, one –NCO group of TDI reacted with Ti–OH of TiO_2 to form the –NHCOOTi bond, through which TDI molecules were anchored on TiO_2 surface to produce the intermediate TP. Subsequently, the unreacted –NCO groups of as-synthesized TP, further reacted with the $-NH_2$ groups of CG to form –NHCONH– bond between TP and CG. As a result, TDI linked together TiO_2 and CG via –NHCOOTi and –NHCONH– bonds to produce a dye-modified TiO_2 (CTP) catalyst. The TDI/TiO_2 molar ratio was crucial to final product CTP. If the molar ratio of TDI/TiO_2 was too low (<0.2), the –NCO groups would be exhausted by Ti–OH groups of TiO_2 surface. The obtained TP had no active –NCO groups on its surface (see Fig. S1 in supporting information) and could not react with $-NH_2$ of dye CG, therefore, CTP could not be obtained. Only when the molar ratio of TDI/TiO_2 was equal to 0.2 or higher, the intermediate TP would have unreacted –NCO groups (see Fig. S1 in supporting information) to further react with TP and synthesize CTP. Thus, TDI/TiO_2 molar ratio 0.2 or higher is necessary to prepare the CTP photocatalysts. As shown by Scheme 1, it was obvious that the dye usage was decided by the TDI dosage. The larger molar ratio of TDI/TiO_2 could lead to the more dye-modification to TiO_2.

3.2. Crystal phase and morphography

XRD patterns of TiO_2, CTP0.2, and CTP0.9 were presented in Fig. 1. It was obviously observed that the XRD patterns of CTP0.2 and CTP0.9 were identical with that of bare TiO_2, indicating that the surface organic modification to TiO_2 had no effect on the crystalline phase. The surface area data of CTP*X* samples were listed in Table 1. From Table 1, it was found the surface area decreased monotonously from 49.96 $m^2 g^{-1}$ of TiO_2 to 32.15 $m^2 g^{-1}$ of CTP0.9 with the increase of *X*. Generally, the decrease in surface area could be attributed to the

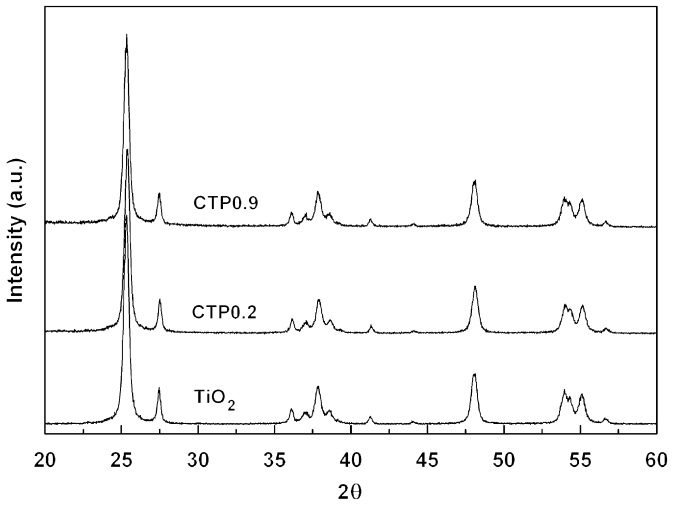

Fig. 1. XRD patterns of bare TiO_2 and dye-modified TiO_2 samples (CTP0.2 and CTP0.9).

Table 1
The surface areas of samples

Samples	TDI/TiO_2 molar ratio	Surface area ($m^2 g^{-1}$)
TiO_2	–	49.96
CTP0.2	0.2	49.73
CTP0.3	0.3	45.44
CTP0.4	0.4	43.26
CTP0.5	0.5	41.48
CTP0.6	0.6	40.61
CTP0.7	0.7	38.56
CTP0.8	0.8	36.25
CTP0.9	0.9	32.15

aggregation between TiO_2 particles. The representative TEM images, shown in Fig. 2, displayed more and more serious aggregation from bare TiO_2 to CTP samples.

3.3. Chemical structure and surface composition

As shown in Scheme 1, two new chemical bonds, including –NHCOOTi and –NHCONH–, came into being during the process of CTP preparation. Therefore, the FT-IR information of these two groups could be used to confirm the CTP chemical structure. The FT-IR spectra of original materials (TDI, CG, and TiO_2), the intermediate (TP0.2) and CTP samples (CTP0.2 and CTP0.9) were given in Fig. 3. In FT-IR spectrum of TDI, a characteristic absorption at 2268 cm^{-1} of –NCO of TDI could be observed and a weak peak at 1602 cm^{-1} is due to the C=C in-plane vibration of the benzene ring. For bare TiO_2, the broad strong peak around 600 cm^{-1} was ascribed to the typical Ti–O–Ti vibration. After TDI was grafted on TiO_2 surface, the obtained TP samples showed an absorption peak at 2268 cm^{-1} suggesting that there were still –NCO groups existing on TP surface, and the narrowing of the peak should be due to the consumption of –NCO of TDI. Simultaneously, new peaks were observed at 1648 and 1228 cm^{-1} (see the FT-IR spectrum of TP0.2), which could be ascribed to the asymmetric stretching vibration and the symmetric stretching vibration of –NHCOOTi, respectively [38]. Because the formation of the π-conjugated –NHCOOTi structure in TP samples (see Scheme 1), here the FT-IR data of –COOTi vibration were lower than the referenced values of –NHCOOTi vibration (1720 and 1270 cm^{-1}) [39]. In the FT-IR spectra of CTP0.2 and CTP0.9, it was found the typical peak of –NCO groups at 2268 cm^{-1} disappeared and a new absorption at 1658 cm^{-1} came into being, compared with the FT-IR spectra of TP0.2 and CG. The disappearance of the band at 2268 cm^{-1} revealed that the –NCO groups were exhausted during chemical reaction between TP samples and CG. The peak at about 1658 cm^{-1} was assigned to the stretching vibration of carbonyl in the structure of –NHCONH– [40]. It must be noticed that the location of –NHCOOTi asymmetric stretching vibration was close to 1658 cm^{-1}, which made the peak broader. Apart from those bands mentioned above, other absorptions at 1539 and 1311 cm^{-1} corresponded to the deformation vibration of N–H and the stretching vibration of N–C, respectively. In conclusion, the newly emerged peaks in FT-IR spectra of CTP samples could well explain the successful modification of dye to the TiO_2 surface via TDI linking.

As the dye modification to TiO_2 only occurred on TiO_2 surface, XPS as a surface characterization technique could be used to investigate the surface element bonding structure of CTP samples. The element composition calculated from the survey XPS analysis, were shown in Table 2. There were only Ti and O elements on the surface of bare TiO_2, but for CTP samples, N and C elements were also intensively detected (see Table 2). Because the as-prepared CTP samples were extracted with CH_2Cl_2 for 48 h, there were hardly unreacted or adsorbed organic compounds on TiO_2 surface. The detected N and C elements should only come from those TDI and CG molecules anchored on TiO_2 surface, which was another evidence for organic molecules modified on TiO_2 surface via chemical bonds. Also from Table 2, the N and C content all increased and the Ti and O content all decreased on CTP samples surface with the rise of organic compounds amount. The increasing organic modification usage could lead to the thicker organic layer on TiO_2 surface. As the measured depths by XPS was about 2–3 nm, it was reasonable that the thicker organic layer was, the less Ti and O content would be detected and reversely the higher N and C contents.

The high-resolution XPS spectra were exhibited in Figs. 4 and 5. In both the O1s region and the Ti2p region of CTP samples, obvious shifts to higher binding energies were observed relative to those of bare TiO_2 (see Fig. 4), which was due to the strong chemical interaction between TiO_2 and organic compounds. The increased binding energies of CTP samples were also good evidences for

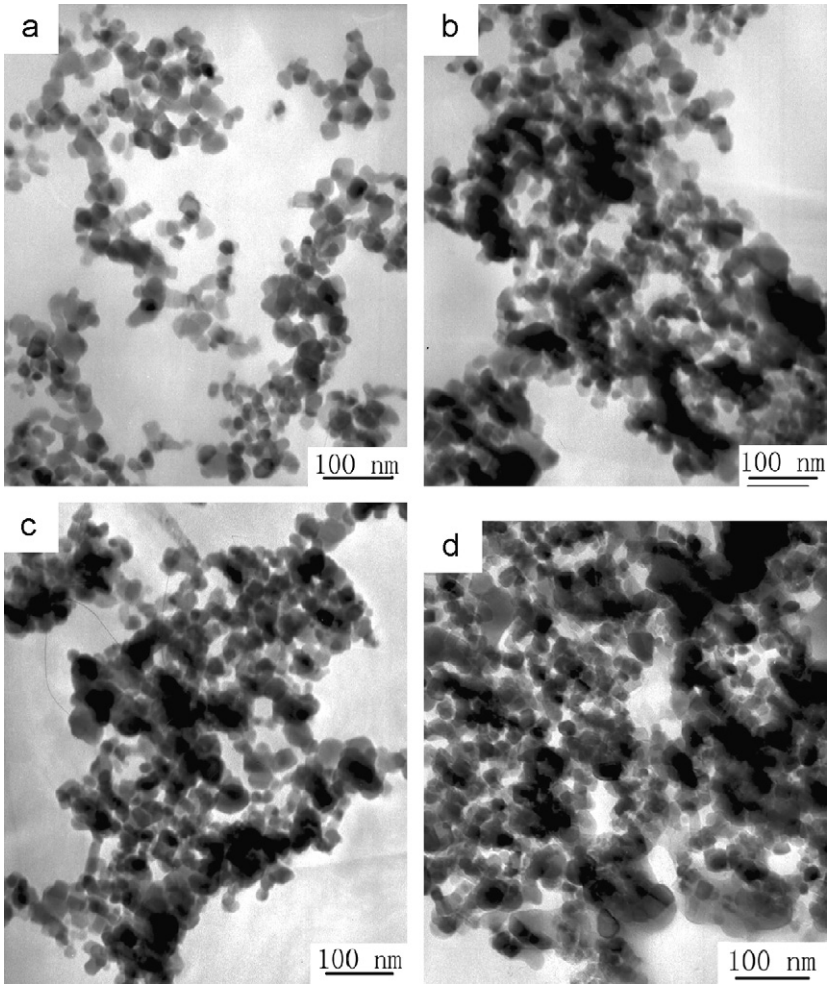

Fig. 2. Typical TEM of bare TiO_2 (a), CTP0.2 (b), CTP0.5 (c), and CTP0.9 (d).

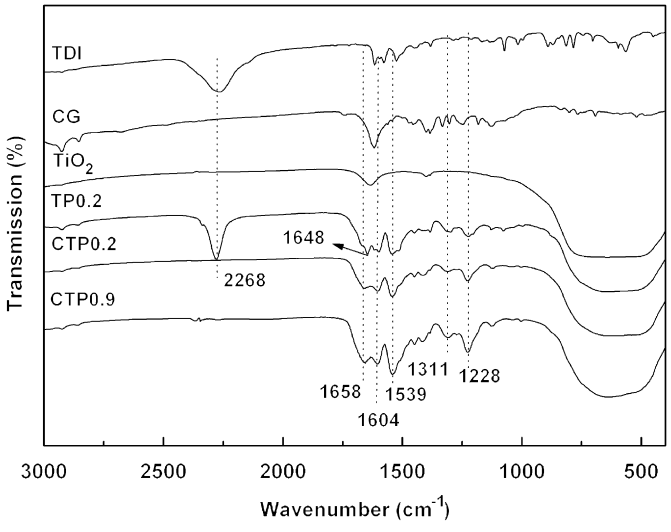

Fig. 3. FT-IR transmission spectra of original materials (TDI, CG, and TiO_2), intermediate TP0.2, and dye-modified TiO_2 (CTP0.2 and CTP0.9).

surface modification of TiO_2 through chemical bonds not adsorption. Shown in Fig. 5, the high-resolution spectra of C1s region were decomposed into three contributions

Table 2
The surface element composition obtained from XPS analysis

Samples	Ti2p (%)	O1s (%)	N1s (%)	C1s (%)
TiO_2	27.87	72.13	–	–
CTP0.2	3.29	27.99	4.82	63.90
CTP0.9	2.34	24.70	8.44	64.52

centered at 285.2, 287.1, and 289.0 eV, which were corresponding to C=C groups in aromatic rings or C–(C/H) groups, C–O or C–N groups, and C=O groups [41], respectively. Because the detected C element only came from those anchored organic compounds (TDI and CG) on TiO_2 surface, these three contributions in C1s XPS spectra should be very useful to explain the surface chemical structure of CTP catalysts.

3.4. UV–vis absorption

To clarify that dye modification to TiO_2 was a useful method to synthesize a visible-activated photocatalyst, it was essential to investigate whether the dye-modified TiO_2

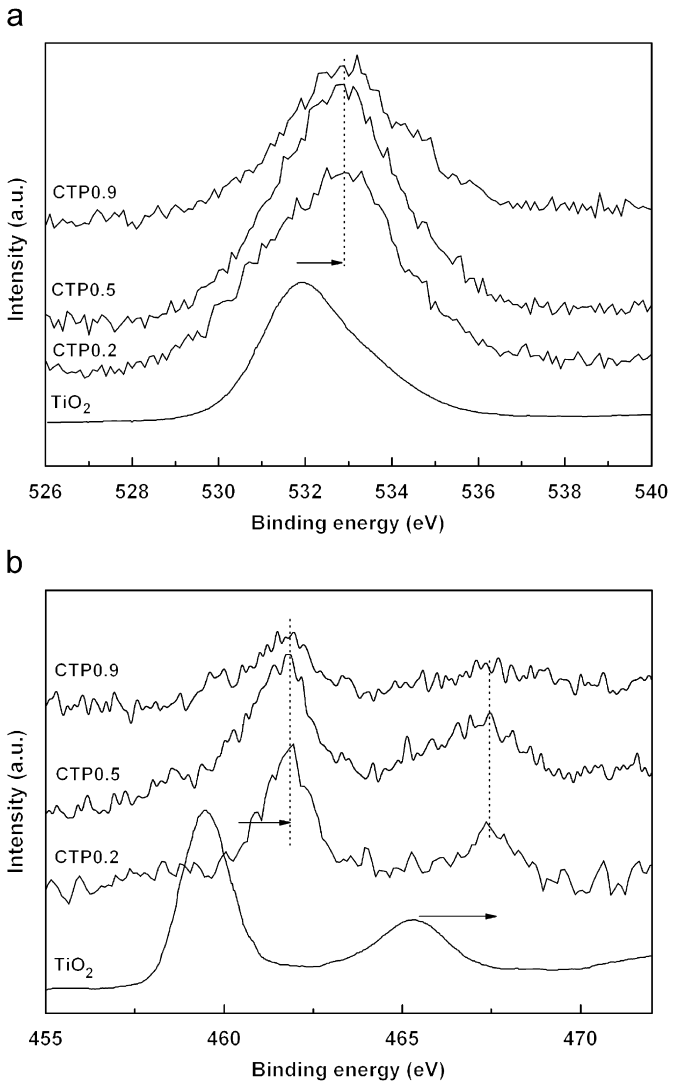

Fig. 4. High-resolution XPS spectra in the O1s region (a) and the Ti2p region (b) for the samples TiO_2, CTP0.2, CTP0.5, and CTP0.9.

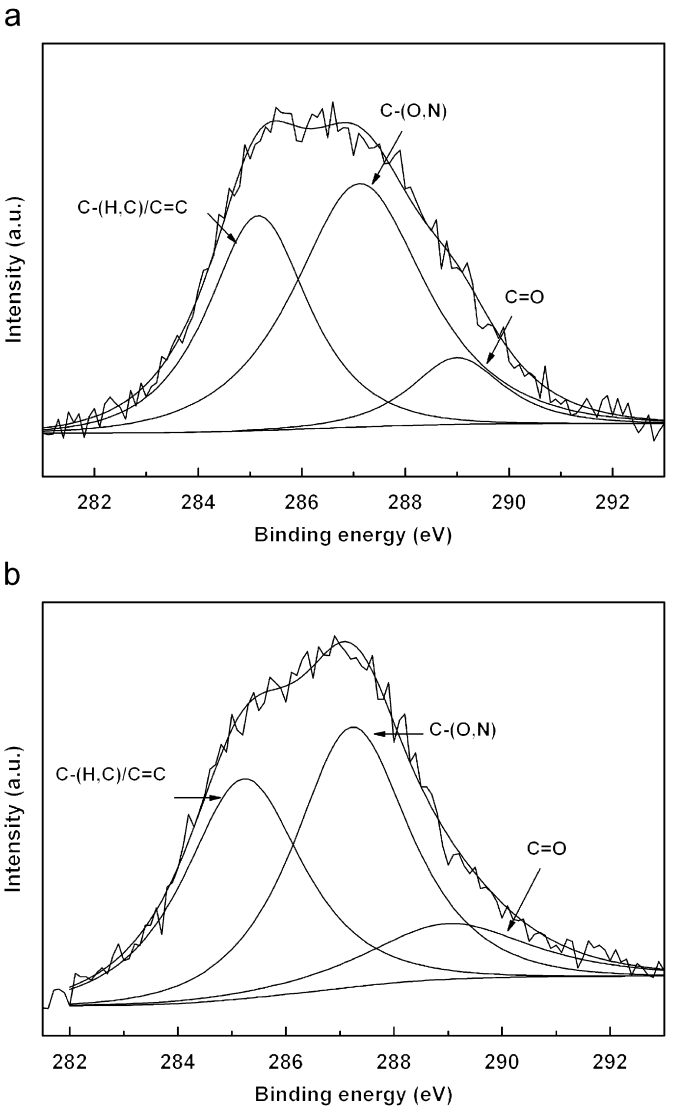

Fig. 5. Fit to the C1s region of the XPS spectrum for CTP0.2 (a) and CTP0.5 (b).

samples could show obvious visible absorption. Fig. 6 showed the UV–vis DRS of bare TiO_2 and CTP samples. From Fig. 6, bare TiO_2 had no visible absorption capability, but dye modification to TiO_2 obviously improved the visible absorption of TiO_2. A distinct and strong absorption centered at 450 nm, which was assigned to intramolecular ligand-to-metal charge transfer transition of complexes on TiO_2 surface [36,37], was observed for every CTP sample (see Fig. 6), and its intensity increased with organic compound content. When the TDI/TiO_2 molar ratio was 0.8 and 0.9, the visible absorption intensity of CTP samples had seldom difference, indicating a saturation of dye modification to TiO_2. The intense visible absorption of CTP samples might be favorable to photocatalysis under visible light irradiation. Additionally, the surface organic complexes on TiO_2 could strongly enhance an interfacial electron-transfer rate, which was also able to improve photocatalytic performance of CTP catalysts [36,37,42].

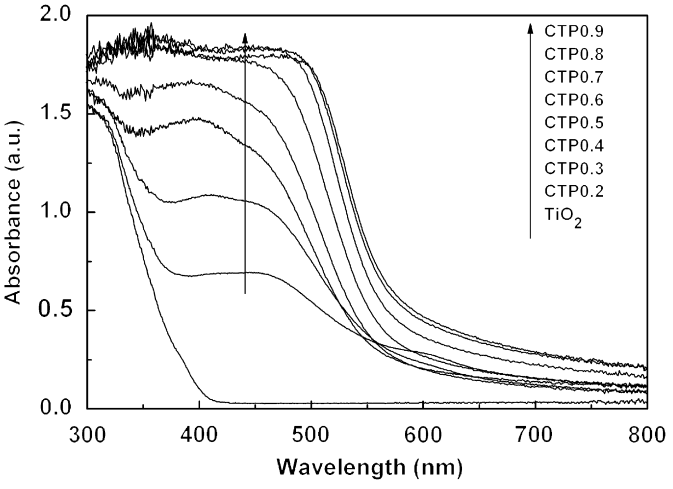

Fig. 6. UV–vis diffuse reflectance spectra of TiO_2 and dye-modified samples.

To further explain why the dye modification to TiO_2 led to intense visible absorption in the range from 400 to 550 nm, the detailed UV–vis spectra including raw materials (TDI, CG, and TiO_2), intermediate TP and CTP samples, were given in Fig. 7a and b. The UV–vis absorption spectra of TDI, TiO_2, and TP samples (TP0.2 and TP0.9) were exhibited in Fig. 7a. It was found that TDI and TiO_2 had no absorption at above 300 and 400 nm, respectively, but TP samples showed obvious red-shifted absorption (see Fig. 7a). Generally, the red-shift meant the decrease of electron-transition energy [43,44], which was decided mainly by chemical structure. As shown in Scheme 1, TP was composed of inorganic Ti atom and organic group –NHCOO–. As a transition-metal element, Ti had unfilled *d*-orbitals, simultaneously; the organic part was an electron-abundant π-conjugated structure. Such TP structure was a typical donor-acceptor type π-conjugated structure, where Ti was the electron acceptor due to the electron-deficient of *d*-orbital and the π-conjugated organic part was the electron donor. This donor-acceptor chemical structure of TP led to the extension of π-conjugation via the electron-deficient *d*-orbital and finally to the decrease of the electron-transition energy [45–47]. Consequently, the photo-induced electron might easily transfer from organic part to inorganic part (ligand-to-metal) and finally resulted in the red-shift in the UV–vis absorption of TP.

Fig. 7b showed the UV–vis spectra of CG, TP (TP0.2 and TP0.9) and CTP samples (CTP0.2 and CTP0.9). As shown in Fig. 7b, the absorption maximum of CG centered at 406 nm. After TP reacted with CG to form CTP, the absorption bands of CTP samples greatly had a red-shift from that of CG. Similar to the above analyses, this obvious red-shift should also be attributed to the decreased electron-transition energy. TP and CG were both π-conjugated structure themselves (see Scheme 1). When TP reacted with CG, the two π-conjugated structures were linked together via another conjugated group –NHCOONH– and produced a bigger π-conjugated structure leading to lower electron-transition energy [47–49]. As a result, CTP samples exhibited much stronger absorption in longer wavelength than all the raw materials and intermediates TP. Due to the bigger π-conjugated structure existing in CTP samples, the electron could more easily transfer from organic part into inorganic one, which was of great significance to improve their photocatalytic performance.

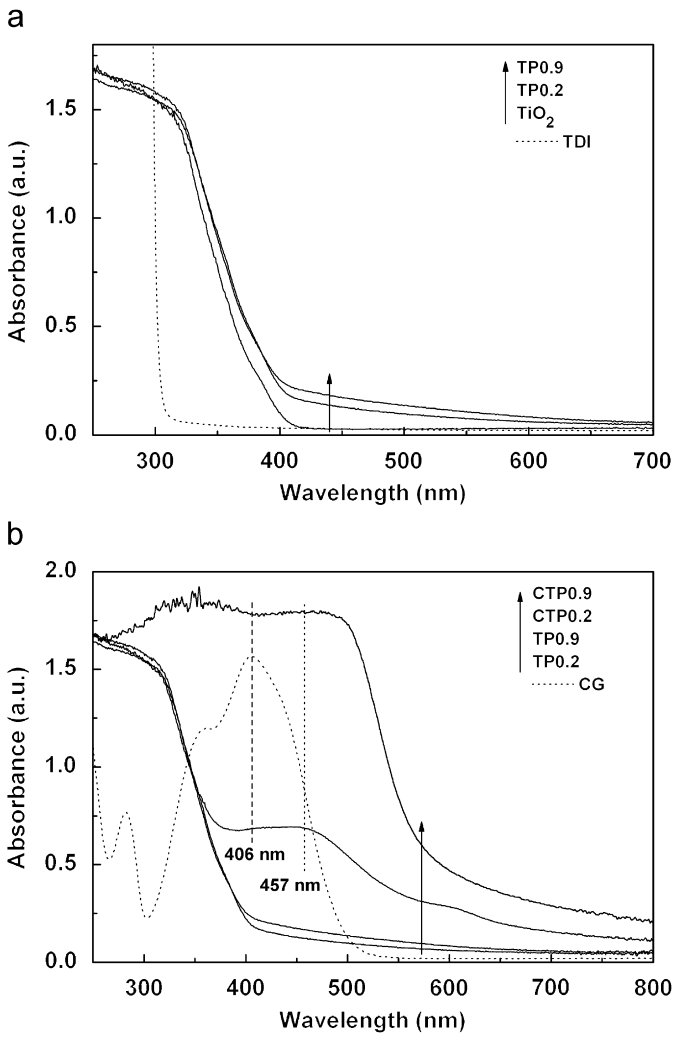

Fig. 7. UV–vis absorption spectra of (a) TDI, TiO_2, TP0.2 and TP0.9, (b) CG, TP0.2, TP0.9, CTP0.2, and CTP0.9.

3.5. Adsorption capacity

The adsorption capacity of CTP catalyst to MB was evaluated by the adsorption amount (C_0-C_e). The higher value of (C_0-C_e) corresponded to the stronger adsorption capacity of catalysts. Fig. 8 showed the adsorption amounts of MB in different molar ratio of TDI/TiO_2. With the increase of the TDI/TiO_2 molar ratio, namely the dye modification amount to TiO_2 gradually enhanced, the adsorption capacity of catalysts exhibited a behavior of 'gradual increase-fast increase to maximum-fast decrease-slow decrease'. It was noticeable that the adsorption

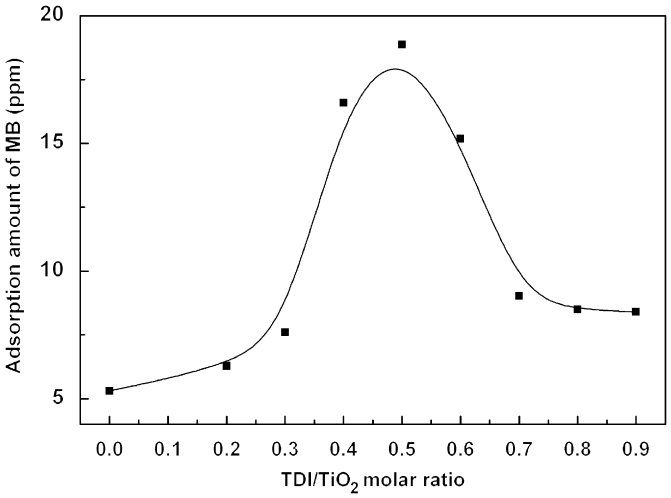

Fig. 8. The adsorption amount in various molar ratio of TDI/TiO_2.

amounts of MB on all CTP catalysts were all higher than that on bare TiO_2 and reached the highest values at TDI/TiO_2 molar ratio 0.5. Another interesting founding was that despite the less surface area, CTP samples had higher adsorption capacity. It was known that the adsorption capacity was mainly determined by two factors: (1) surface area of catalyst, (2) surface chemical property of catalyst. Undoubtedly, less surface area would not benefit adsorption. In contrast, the surface organic modification to TiO_2 should improve the chemical compatibility between TiO_2 and MB to enhance the MB adsorption [48]. As a combined result, it was understandable that CTP catalysts had higher MB adsorption capacity than bare TiO_2. But, when the TDI/TiO_2 molar ratio is beyond 0.5, the adsorption capacity of CTP samples largely decreased. To explain the decline of adsorption capacity, another factor, the steric hindrance effect, must be considered here. As is well known, when the surface organic complexes increased to a certain extent, the steric hindrance effect became obvious and held back MB adsorption on dye-modified TiO_2 [49]. Therefore, it was acceptable that the adsorption capacity underwent a decline when the TDI/TiO_2 molar ratio is higher than 0.5. The maximum adsorption capacity of CTP0.5 should be a balanced result between surface area, chemical compatibility of surface modification to MB, and the steric hindrance effect.

3.6. Photodegradation of methylene blue (MB)

Based on the above analyses, it could be concluded that the dye modification to TiO_2 not only could make TiO_2 show strong visible absorption but also enhance its adsorption capacity to MB. Therefore, the dye-modified TiO_2 should exhibit improved visible photocatalytic activity compared with bare TiO_2. For comparison, two blank experiments were carried out, including one under visible-irradiation without catalysts and another in the dark with catalysts. Both of them showed no MB degradation.

The photocatalytic performances of catalysts (bare TiO_2 and CTP samples) were evaluated with the photodegradation percentage to MB after 12-h irradiation under visible light. To clearly compare the photocatalytic performances of various catalysts, the photodegradation percentage in different TDI/TiO_2 molar ratio was shown in Fig. 9. It was found that bare TiO_2 showed very poor photocatalytic activity, but CTP photocatalysts exhibited notably high reactivity. It was generally thought that the photocatalytic performance depended on the phase structure, the absorbance [50,51], and the adsorption capacity [52,53] of photocatalyst. In our experiments, all photocatalysts were identical anatase phase, so the different phtocatalytic activity should depend on the latter two factors. Due to the far more intense absorbance in visible region and higher adsorption capacity of CTP catalysts than that of bare TiO_2, it was reasonable that CTP catalysts showed much better photocatalytic activity than bare TiO_2. In addition, another important founding from Fig. 9 was that with the increase of TDI/TiO_2 molar ratios from 0.2 to 0.9, the photocatalytic performance firstly increased and then decreased. On the whole, the change trend of photocatalytic performance was in agreement with that of MB adsorption capacity, indicating the photocatalytic activities of CTP catalysts were mainly decided by their adsorption capacity. However, the decreasing trend shown in Fig. 8 was different as the molar ratio of TDI/TiO_2 > 0.5. The adsorption capacity from CTP0.5 to CTP0.9 had a rapidly decline, and that the photocatalytic activity decreased slowly. This difference should be attributed to two co-operating factors, including the increasing absorbance (positive factor) and the decreasing adsorption capacity (negative factor). When the TDI/TiO_2 molar ratio was higher than 0.5, the visible absorbance was gradually enhanced but the adsorption capacity was quickly reduced. So, the photocatalytic performance exhibited a slow decline as the molar ratio of TDI/TiO_2 > 0.5.

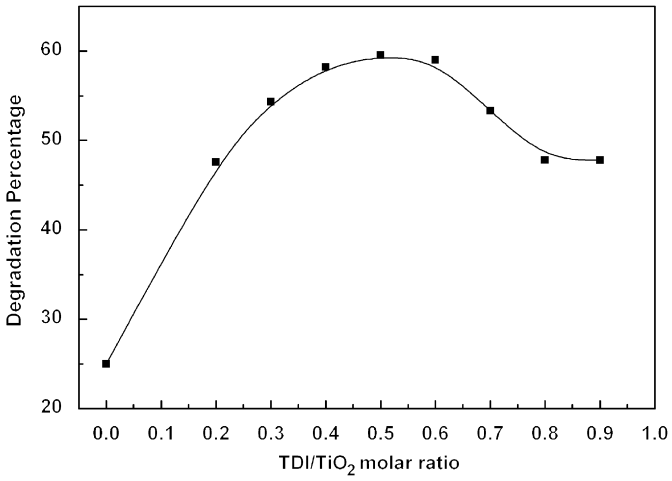

Fig. 9. The photodegradation percentage at 12-h reaction as a function of different TDI/TiO_2 molar ratio.

3.7. Stability of catalysts

As a representative photocatalyst, CTP0.5 was investigated under 24-h visible light irradiation in aqueous–ethanol suspension without MB to study its photostability. It was found that no considerable change was observed in the FT-IR and UV–vis DRS of CTP0.5 before and after visible light irradiation (see Figs. S2 and S3 in supporting information), which indicated CTP0.5 was very photostable. In addition, an examination to the recycled photocatalytic activity of CTP0.5 was also carried out, and the corresponding result was presented in Fig. 10. It was found that twice-recycled CTP0.5 catalyst exhibited a photocatalytic activity similar to that of the fresh CTP0.5. Based on the above results, the CTP catalysts were photostable.

3.8. Mechanism of photodegradation

MB can undergo photodegradation under visible irradiation in aqueous TiO_2 suspension, which not only led to photobleaching but also causes a complete decomposition of MB into CO_2 [54,55]. The photodegradation pathway under visible irradiation is different from that under UV light for TiO_2 suspension. Herein, the possible mechanism of photocatalytic decomposition of MB over dye-modified TiO_2 under visible light was also discussed (see Fig. 11). The modification of dye to TiO_2 led to form donor-acceptor type π-conjugated surface complexes on TiO_2 surface that could be easily excited by visible light. The electrons excited from π-conjugated surface complexes (donor) would inject into the unfilled *d*-orbital of Ti (acceptor), and then transferred into conduction band of TiO_2. As a result, the surface complex became cationic radical. Simultaneously, the MB molecules absorbed on the surface complex could transfer electrons into the cationic radical of surface complex and generated MB^+ (see Fig. 11). MB^+ was essential to further photocatalytic reaction. Those electrons of TiO_2 conduction band were captured by the O_2 preadsorbed on TiO_2 surface to form superoxide anion radical ($O_2^{\bullet -}$), which further converted to hydrogen peroxide radicals ($HOO^\bullet$) and hydroxyl radicals ($HO^\bullet$) via a series of protonation, disproportionation and reduction steps. The hydroxyl radicals were proposed to be the primary oxidant in the photocatalytic reaction. Finally, the hydroxyl radicals reacted with MB^+ molecules to produce the degradation product [56]. Noticeably, since MB could absorb visible light itself, it could inevitably act as a sensitizer for TiO_2. Generally, it was necessary to the aim of photocatalytic sensitization that MB must adsorb on TiO_2 surface. Moreover, the larger the adsorption amount was, the stronger the sensitization effect of MB to TiO_2 was. For dye-modified TiO_2, because the TiO_2 surface was covered by dye molecules, the amount of MB directly contacting with TiO_2 decreased with the enhanced dye modification. Thus, the MB sensitization effect to TiO_2 was greatly weakened for dye-modified TiO_2. As a result, the obviously improved visible photocatalytic activity of dye-modified TiO_2 should mainly be attributed to the dye modification to TiO_2, not the sensitization effect of MB to TiO_2.

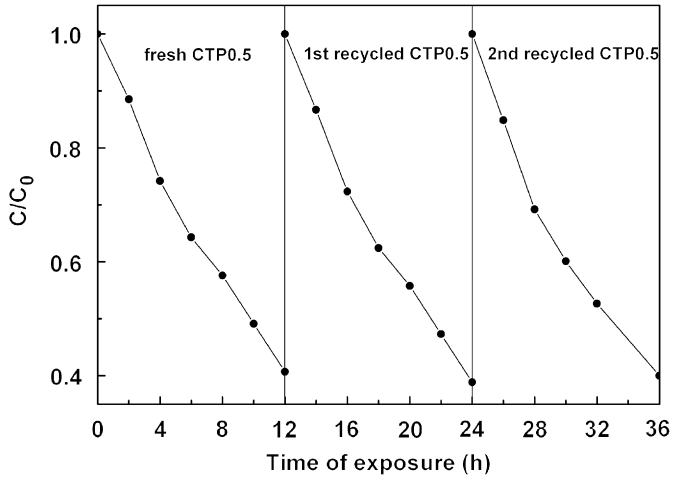

Fig. 10. Photocatalytic degradation of MB with recycled CTP0.5.

4. Conclusion

Dye-modified TiO_2 photocatalysts were prepared by chemical reactions between dye, TDI and TiO_2 with TDI as a bridging molecule. The dye modification to TiO_2 led to strong absorption in visible region and enhanced adsorption capacity to MB. As a result, dye-modified TiO_2 samples showed higher visible photocatalytic activity than bare TiO_2 for the degradation of MB. For the photocatalysts presented in this work, there were mainly three factors affecting photocatalytic activity, including phase structure, absorbance and adsorption capacity. Among all the samples, CTP0.5 exhibited best photocatalytic activity under visible light irradiation due to the strongest adsorption capacity and higher absorbance in visible

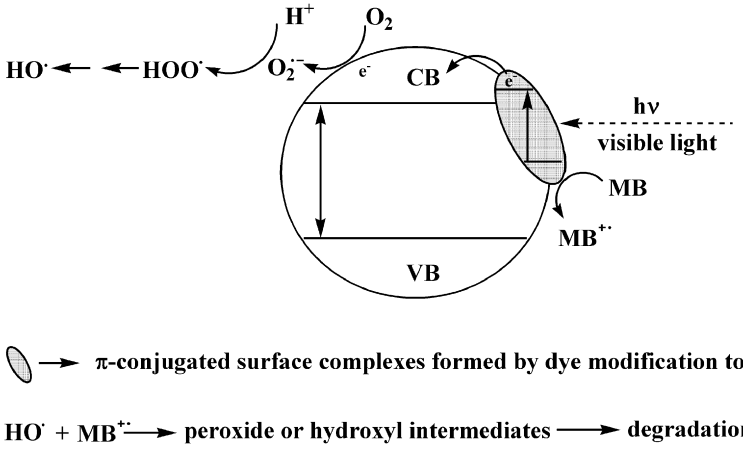

Fig. 11. The mechanism of photocatalytic decomposition of MB over dye-modified TiO_2 under visible light.

region. The dye-modified TiO_2 photocatalysts also showed good stability under visible light irradiation.

Acknowledgment

The financial support from Shanxi Natural Science Foundations (Nos. 20051025, 2006021031, and 2007021014) was acknowledged.

Appendix A. Supplementary materials

Supplementary data associated with this article can be found in the online version at doi:10.1016/j.jssc.2008.01.004.

References

[1] A.L. Linsebigler, G.Q. Lu, J.T. Yates Jr., Chem. Rev. 95 (1995) 735–758.
[2] S. Yin, Q.W. Zhang, F. Saito, T. Sato, Chem. Lett. 32 (2003) 358–359.
[3] J. Zhou, M. Takeuchi, A.K. Ray, M. Anpo, X.S. Zhao, J. Colloid Interface Sci. 311 (2007) 497–501.
[4] H. Kisch, L. Zang, C. Lange, W.F. Maier, C. Antonius, D. Meissner, Angew. Chem., Int. Ed. 37 (1998) 3034–3036.
[5] L. Zang, C. Lange, I. Abraham, S. Storck, W.F. Maier, H. Kisch, J. Phys. Chem. B 102 (1998) 10765–10771.
[6] H. Yamashita, Y. Ichihashi, M. Takeuchi, S. Kishiguchi, M. Anpo, J. Synchrotron Radiat. 6 (1999) 451–452.
[7] M. Anpo, M. Takeuchi, Int. J. Photoenergy 3 (2001) 89–94.
[8] L. Zang, W. Macyk, C. Lange, W.F. Maier, C. Antonius, D. Meissner, H. Kisch, Chem. Eur. J. 6 (2000) 379–384.
[9] H. Yamashita, M. Harada, J. Misaka, M. Takeuchi, B. Neppolian, M. Anpo, Catal. Today 84 (2003) 191–196.
[10] M. Iwasaki, M. Hara, H. Kawada, H. Tada, S. Ito, J. Colloid Interface Sci. 224 (2000) 202–204.
[11] W. Choi, A. Termin, M.R. Hoffmann, J. Phys. Chem. 98 (1994) 13669–13679.
[12] H. Yamashita, M. Honda, M. Harada, Y. Ichihashi, M. Anpo, T. Hirao, N. Itoh, N. Iwamoto, J. Phys. Chem. B 102 (1998) 10707–10711.
[13] S. Khan, M. Al-Shahry, W.B. Ingler, Science 297 (2002) 2243–2245.
[14] C. Lettmann, K. Hildenbrand, H. Kisch, W. Macyk, W.F. Maier, Appl. Catal. B: Environ. 32 (2001) 215–227.
[15] H. Kisch, S. Sakthivel, M. Janczarek, D. Mitoraj, J. Phys. Chem. C 111 (2007) 11445–11449.
[16] B. Neumann, P. Bogdanoff, H. Tributsch, S. Sakthivel, H. Kisch, J. Phys. Chem. B 109 (2005) 16579–16586.
[17] S. Sakthivel, M. Janczarek, H. Kisch, J. Phys. Chem. B 108(2004) 19384–19387.
[18] S. Sakthivel, H. Kisch, Angew. Chem. Int. Ed. 42 (2003) 4908–4911.
[19] S. Sakthivel, H. Kisch, Chemphyschem 4 (2003) 487–490.
[20] R. Asahi, T. Morikawa, T. Ohwaki, A. Aoki, Y. Taga, Science 293 (2001) 269–271.
[21] Y. Kuroda, T. Mori, K. Yagi, N. Makihata, Y. Kawahara, M. Nagao, S. Kittaka, Langmuir 21 (2005) 8026–8034.
[22] H. Irie, Y. Watanabe, K. Hashimoto, J. Phys. Chem. B 107 (2003) 5483–5486.
[23] C. Burda, Y.B. Lou, X.B. Chen, A.C.S. Samia, J. Stout, J.L. Gole, Nano Lett. 3 (2003) 1049–1051.
[24] T. Umebayashi, T. Yamaki, H. Itoh, K. Asai, Appl. Phys. Lett. 81 (2002) 454–456.
[25] D.B. Hamal, K.J. Klabunde, J. Colloid Interface Sci. 311 (2007) 514–522.
[26] J. Wang, S. Yin, Q. Zhang, F. Saito, T. Sato, Chem. Lett. 32 (2003) 540–541.
[27] W. Zhao, W. Ma, C. Chen, J. Zhao, Z. Shuai, J. Am. Chem. Soc. 126 (2004) 4782–4783.
[28] X. Hong, Z. Wang, W. Cai, F. Lu, J. Zhang, Y. Yang, N. Ma, Y. Liu, Chem. Mater. 17 (2005) 1548–1552.
[29] D. Li, H. Haneda, S. Hishita, N. Ohashi, Chem. Mater. 17 (2005) 2588–2595.
[30] D. Li, N. Ohashi, S. Hishita, T. Kolodiazhnyi, H. Haneda, J. Solid State Chem. 178 (2005) 3293–3302.
[31] J. Moon, C. Yun, K. Chung, M. Kang, J. Yi, Catal. Today 87 (2003) 77–86.
[32] D. Chatterjee, A. Mahata, Appl. Catal. B: Environ. 33 (2001) 119–125.
[33] M.R. Hoffmann, S.T. Martin, W. Choi, D.W. Bahnemannt, Chem. Rev. 95 (1995) 69–96.
[34] Y. Liu, J.I. Dadap, D. Zimdars, K.B. Eisenthal, J. Phys. Chem. B 103 (1999) 2480–2486.
[35] J. Moser, S. Punchihewa, P.P. Infelta, M. Grätzel, Langmuir 7 (1991) 3012–3018.
[36] A.E. Regazzoni, P. Mandelbaum, M. Matsuyoshi, S. Schiller, S.A. Bilmes, M.A. Blesa, Langmuir 14 (1998) 868–874.
[37] S. Ikeda, C. Abe, T. Torimoto, B. Ohtani, J. Photochem. Photobiol. A: Chem. 160 (2003) 61–67.
[38] D. Jiang, Y. Xu, B. Hou, D. Wu, Y. Sun, J. Solid State Chem. 180 (2007) 1787–1791.
[39] S. Doeuff, M. Henry, C. Sanchez, J. Livage, J. Non-Cryst. Solids 89 (1987) 206–212.
[40] A. Kohut, A. Voronov, W. Peukert, Langmuir (2007) 504–508.
[41] S. Biniak, G. Szymanskj, J. Siedlewskj, A. Swiatkowski, Carbon 35 (1997) 1799–1810.
[42] T. Rajh, J.M. Nedeljkovic, L.X. Chen, O. Poluektov, M.C. Thurnauer, J. Phys. Chem. B 103 (1999) 3515–3519.
[43] M.K. Nazeeruddin, R. Humphry-Baker, P. Liska, M. Grätzel, J. Phys. Chem. B 127 (2003) 8981–8987.
[44] S. Braverman, D. Cohen, D. Reisman, H. Basch, J. Am. Chem. Soc. 102 (1980) 6656–6658.
[45] N. Matsumi, Y. Chujo, O. Lavastre, P.H. Dixneuf, Organometallics 20 (2001) 2426–2427.
[46] B.S. Lele, A.J. Russell, Biomacromolecules 5 (2004) 1947–1955.
[47] N. Matsumi, Y. Chujo, Macromolecules 33 (2000) 8146–8148.
[48] H. Park, W. Choi, J. Phys. Chem. B 109 (2005) 11667–11674.
[49] Y.K. Gong, K. Nakashima, J. Phys. Chem. B 106 (2002) 803–808.
[50] B. Zielinska, J. Grzechulska, B. Grzmil, A.W. Morawski, Appl. Catal. B: Environ. 35 (2001) L1–L7.
[51] B. Ohtani, Y. Ogawa, S. Nishimoto, J. Phys. Chem. B 101 (1997) 3746–3752.
[52] C. Minero, F. Catozzo, E. Pelizzetti, Langmuir 8 (1992) 481–486.
[53] C. Kormann, D.W. Bahnemann, M.R. Hoffmann, Environ. Sci. Technol. 25 (1991) 494–500.
[54] J. Zhao, K. Wu, H. Hidaka, N. Serpone, J. Chem. Soc. Faraday Trans. 94 (1998) 673–676.
[55] F. Zhang, J. Zhao, L. Zang, T. Shen, H. Hidaka, E. Pelizzetti, N. Serpone, Appl. Catal. B: Environ. 15 (1998) 147–156.
[56] T. Wu, T. Lin, J. Zhao, H. Hidaka, N. Serpone, Environ. Sci. Techonl. 33 (1999) 1379–1387.